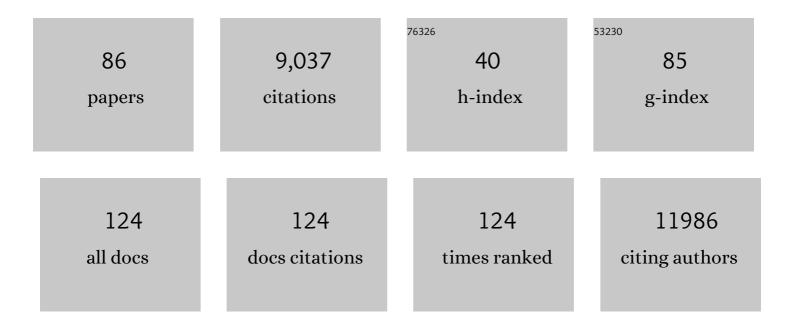
List of Publications by Year in descending order

Source: https://exaly.com/author-pdf/9478646/publications.pdf Version: 2024-02-01



#	Article	IF	CITATIONS
1	Transcriptional regulation by calcium, calcineurin, and NFAT. Genes and Development, 2003, 17, 2205-2232.	5.9	1,675
2	FOXP3 Controls Regulatory T Cell Function through Cooperation with NFAT. Cell, 2006, 126, 375-387.	28.9	1,019
3	DNA Binding Site Sequence Directs Glucocorticoid Receptor Structure and Activity. Science, 2009, 324, 407-410.	12.6	618
4	Structure of the DNA-binding domains from NFAT, Fos and Jun bound specifically to DNA. Nature, 1998, 392, 42-48.	27.8	498
5	The crystal structure of Haelll methyltransferase covalently complexed to DNA: An extrahelical cytosine and rearranged base pairing. Cell, 1995, 82, 143-153.	28.9	399
6	Crystal structure of the extracellular domain of nAChR α1 bound to α-bungarotoxin at 1.94 Ã resolution. Nature Neuroscience, 2007, 10, 953-962.	14.8	398
7	Docking Motif Interactions in MAP Kinases Revealed by Hydrogen Exchange Mass Spectrometry. Molecular Cell, 2004, 14, 43-55.	9.7	278
8	Direct identification of the active-site nucleophile in a DNA (cytosine-5)-methyltransferase. Biochemistry, 1991, 30, 11018-11025.	2.5	245
9	Solution Structure of Prosurvival Mcl-1 and Characterization of Its Binding by Proapoptotic BH3-only Ligands. Journal of Biological Chemistry, 2005, 280, 4738-4744.	3.4	187
10	Ligand-binding domain of an α7-nicotinic receptor chimera and its complex with agonist. Nature Neuroscience, 2011, 14, 1253-1259.	14.8	183
11	Population-based 3D genome structure analysis reveals driving forces in spatial genome organization. Proceedings of the National Academy of Sciences of the United States of America, 2016, 113, E1663-72.	7.1	182
12	Structure of the Forkhead Domain of FOXP2 Bound to DNA. Structure, 2006, 14, 159-166.	3.3	176
13	Structure of a Domain-Swapped FOXP3 Dimer on DNA and Its Function in Regulatory T Cells. Immunity, 2011, 34, 479-491.	14.3	140
14	Species-Specific Deamidation of cGAS by Herpes Simplex Virus UL37 Protein Facilitates Viral Replication. Cell Host and Microbe, 2018, 24, 234-248.e5.	11.0	140
15	Crystal Structure of the p53 Core Domain Bound to a Full Consensus Site as a Self-Assembled Tetramer. Structure, 2010, 18, 246-256.	3.3	129
16	A Distal Enhancer in the Interferon-γ (IFN-γ) Locus Revealed by Genome Sequence Comparison. Journal of Biological Chemistry, 2004, 279, 4802-4810.	3.4	123
17	Nicotinic acetylcholine receptor agonist attenuates ILC2-dependent airway hyperreactivity. Nature Communications, 2016, 7, 13202.	12.8	108
18	Structure of a TonEBP–DNA complex reveals DNA encircled by a transcription factor. Nature Structural Biology, 2002, 9, 90-94.	9.7	106

#	Article	IF	CITATIONS
19	Unusual Rel-like architecture in the DNA-binding domain of the transcription factor NFATc. Nature, 1997, 385, 172-176.	27.8	103
20	Mechanism of Recruitment of Class II Histone Deacetylases by Myocyte Enhancer Factor-2. Journal of Molecular Biology, 2005, 345, 91-102.	4.2	100
21	Sequence-specific recruitment of transcriptional co-repressor Cabin1 by myocyte enhancer factor-2. Nature, 2003, 422, 730-734.	27.8	99
22	DNA Binding by GATA Transcription Factor Suggests Mechanisms of DNA Looping and Long-Range Gene Regulation. Cell Reports, 2012, 2, 1197-1206.	6.4	94
23	Structure of NFAT1 bound as a dimer to the HIV-1 LTR κB element. Nature Structural and Molecular Biology, 2003, 10, 800-806.	8.2	92
24	Structural, Biochemical, and Functional Analyses of CED-9 Recognition by the Proapoptotic Proteins EGL-1 and CED-4. Molecular Cell, 2004, 15, 999-1006.	9.7	92
25	Crystal Structures of Multiple GATA Zinc Fingers Bound to DNA Reveal New Insights into DNA Recognition and Self-Association by GATA. Journal of Molecular Biology, 2008, 381, 1292-1306.	4.2	88
26	DNA methylation through a locally unpaired intermediate. Journal of the American Chemical Society, 1993, 115, 12583-12584.	13.7	85
27	Complex between α-bungarotoxin and an α7 nicotinic receptor ligand-binding domain chimaera. Biochemical Journal, 2013, 454, 303-310.	3.7	73
28	Crystal structure of a conserved N-terminal domain of histone deacetylase 4 reveals functional insights into glutamine-rich domains. Proceedings of the National Academy of Sciences of the United States of America, 2007, 104, 4297-4302.	7.1	70
29	Structural Basis of HIV-1 Activation by NF-κB—A Higher-Order Complex of p50:RelA Bound to the HIV-1 LTR. Journal of Molecular Biology, 2009, 393, 98-112.	4.2	69
30	Combinatorial gene regulation by eukaryotic transcription factors. Current Opinion in Structural Biology, 1999, 9, 48-55.	5.7	66
31	Mutational separation of DNA binding from catalysis in a DNA cytosine methyltransferase. Journal of the American Chemical Society, 1993, 115, 5318-5319.	13.7	64
32	Structure of p53 binding to the BAX response element reveals DNA unwinding and compression to accommodate base-pair insertion. Nucleic Acids Research, 2013, 41, 8368-8376.	14.5	64
33	Only one of the two DNA-bound orientations of AP-1 found in solution cooperates with NFATp. Current Biology, 1995, 5, 882-889.	3.9	63
34	An asymmetric NFAT1 dimer on a pseudo-palindromic κB-like DNA site. Nature Structural and Molecular Biology, 2003, 10, 807-811.	8.2	56
35	Structure of p300 bound to MEF2 on DNA reveals a mechanism of enhanceosome assembly. Nucleic Acids Research, 2011, 39, 4464-4474.	14.5	53
36	DNA binding by FOXP3 domain-swapped dimer suggests mechanisms of long-range chromosomal interactions. Nucleic Acids Research, 2015, 43, 1268-1282.	14.5	49

#	Article	IF	CITATIONS
37	Demonstration of the in vivo interaction of key cell death regulators by structure-based design of second-site suppressors. Proceedings of the National Academy of Sciences of the United States of America, 2000, 97, 11916-11921.	7.1	46
38	A multifunctional plasmid for protein expression by ECPCR: overproduction of the p50 subunit of NF-κB. Bioorganic and Medicinal Chemistry Letters, 1993, 3, 1089-1094.	2.2	44
39	Inhibition of the function of class IIa HDACs by blocking their interaction with MEF2. Nucleic Acids Research, 2012, 40, 5378-5388.	14.5	44
40	Limited proteolysis and site-directed mutagenesis of the NF-κB p50 DNA-binding subunit. Bioorganic and Medicinal Chemistry Letters, 1993, 3, 1095-1100.	2.2	42
41	Structure of the MADS-box/MEF2 Domain of MEF2A Bound to DNA and Its Implication for Myocardin Recruitment. Journal of Molecular Biology, 2010, 397, 520-533.	4.2	42
42	Conserved forkhead dimerization motif controls DNA replication timing and spatial organization of chromosomes in <i>S. cerevisiae</i> . Proceedings of the National Academy of Sciences of the United States of America, 2017, 114, E2411-E2419.	7.1	40
43	Structure of the Forkhead Domain of FOXA2 Bound to a Complete DNA Consensus Site. Biochemistry, 2017, 56, 3745-3753.	2.5	39
44	Mining 3D genome structure populations identifies major factors governing the stability of regulatory communities. Nature Communications, 2016, 7, 11549.	12.8	36
45	Structural basis for DNA recognition by FOXC2. Nucleic Acids Research, 2019, 47, 3752-3764.	14.5	36
46	A Cytokine–Cytokine Interaction in the Assembly of Higher-Order Structure and Activation of the Interleukine-3:Receptor Complex. PLoS ONE, 2009, 4, e5188.	2.5	36
47	Structural insight into the molecular mechanism of p53-mediated mitochondrial apoptosis. Nature Communications, 2021, 12, 2280.	12.8	33
48	Reversal of pathological cardiac hypertrophy via the MEF2-coregulator interface. JCI Insight, 2017, 2, .	5.0	33
49	Structure of NFAT Bound to DNA as a Monomer. Journal of Molecular Biology, 2003, 334, 1009-1022.	4.2	32
50	The Cancer Mutation D83V Induces an α-Helix to β-Strand Conformation Switch in MEF2B. Journal of Molecular Biology, 2018, 430, 1157-1172.	4.2	31
51	The Sir4 C-terminal Coiled Coil is Required for Telomeric and Mating Type Silencing in Saccharomyces cerevisiae. Journal of Molecular Biology, 2003, 334, 769-780.	4.2	29
52	Crystal Structure of NFAT Bound to the HIV-1 LTR Tandem κB Enhancer Element. Structure, 2008, 16, 684-694.	3.3	29
53	Mechanism of forkhead transcription factors binding to a novel palindromic DNA site. Nucleic Acids Research, 2021, 49, 3573-3583.	14.5	28
54	[7] Overproduction of proteins using expression-cassette polymerase chain reaction. Methods in Enzymology, 1993, 217, 79-102.	1.0	26

#	Article	IF	CITATIONS
55	p53 destabilizing protein skews asymmetric division and enhances NOTCH activation to direct self-renewal of TICs. Nature Communications, 2020, 11, 3084.	12.8	26
56	Synthesis of an oligonucleotide suicide substrate for DNA methyltransferases. Journal of Organic Chemistry, 1992, 57, 2989-2991.	3.2	25
57	A Negatively Charged Amino Acid in Skp2 Is Required for Skp2-Cks1 Interaction and Ubiquitination of p27Kip1. Journal of Biological Chemistry, 2003, 278, 32390-32396.	3.4	24
58	Conformations of p53 response elements in solution deduced using site-directed spin labeling and Monte Carlo sampling. Nucleic Acids Research, 2014, 42, 2789-2797.	14.5	23
59	Structural basis of binding of homodimers of the nuclear receptor NR4A2 to selective Nur-responsive DNA elements. Journal of Biological Chemistry, 2019, 294, 19795-19803.	3.4	23
60	In Search of Allosteric Modulators of α7-nAChR by Solvent Density Guided Virtual Screening. Journal of Biomolecular Structure and Dynamics, 2011, 28, 695-715.	3.5	22
61	Signal Integration by Transcription-factor Assemblies: Interactions of NF-AT1 and AP-1 on the IL-2 Promoter. Cold Spring Harbor Symposia on Quantitative Biology, 1999, 64, 527-532.	1.1	22
62	Structural insights into the molecular mechanisms of myasthenia gravis and their therapeutic implications. ELife, 2017, 6, .	6.0	22
63	In pursuit of the high-resolution structure of nicotinic acetylcholine receptors. Journal of Physiology, 2010, 588, 557-564.	2.9	20
64	Structural Determinants for α-Neurotoxin Sensitivity in Muscle nAChR and Their Implications for the Gating Mechanism. Channels, 2007, 1, 234-237.	2.8	19
65	Packing of the Extracellular Domain Hydrophobic Core Has Evolved to Facilitate Pentameric Ligand-gated Ion Channel Function. Journal of Biological Chemistry, 2011, 286, 3658-3670.	3.4	18
66	Landscape of DNA binding signatures of myocyte enhancer factor-2B reveals a unique interplay of base and shape readout. Nucleic Acids Research, 2020, 48, 8529-8544.	14.5	17
67	Inter-residue coupling contributes to high-affinity subtype-selective binding of α-bungarotoxin to nicotinic receptors. Biochemical Journal, 2013, 454, 311-321.	3.7	16
68	Acetylation-mediated degradation of HSD17B4 regulates the progression of prostate cancer. Aging, 2020, 12, 14699-14717.	3.1	16
69	Molecular and Biochemical Characterization of the Skp2-Cks1 Binding Interface. Journal of Biological Chemistry, 2004, 279, 51362-51369.	3.4	13
70	Remarkably Stereospecific Utilization of ATP α,β-Halomethylene Analogues by Protein Kinases. Journal of the American Chemical Society, 2017, 139, 7701-7704.	13.7	13
71	Crystallization and Preliminary Crystallographic Analysis of a DNA (Cytosine-5)-Methyltransferase from Haemophilus aegyptius Bound Covalently to DNA. Journal of Molecular Biology, 1994, 238, 626-629.	4.2	12
72	DNA-binding properties of FOXP3 transcription factor. Acta Biochimica Et Biophysica Sinica, 2017, 49, 792-799.	2.0	12

#	Article	IF	CITATIONS
73	Crystal Structure of Apo MEF2B Reveals New Insights in DNA Binding and Cofactor Interaction. Biochemistry, 2018, 57, 4047-4051.	2.5	11
74	Selective base-pair destabilization enhances binding of a DNA methyltransferase. Tetrahedron, 1997, 53, 12041-12056.	1.9	9
75	α1-FANGs: Protein Ligands Selective for the α-Bungarotoxin Site of the α1-Nicotinic Acetylcholine Receptor. ACS Chemical Biology, 2018, 13, 2568-2576.	3.4	8
76	Dissection of Anti-tumor Activity of Histone Deacetylase Inhibitor SAHA in Nasopharyngeal Carcinoma Cells via Quantitative Phosphoproteomics. Frontiers in Cell and Developmental Biology, 2020, 8, 577784.	3.7	7
77	A small molecular compound CC1007 induces cross-lineage differentiation by inhibiting HDAC7 expression and HDAC7/MEF2C interaction in BCR-ABL1â° pre-B-ALL. Cell Death and Disease, 2020, 11, 738.	6.3	6
78	Expression and purification of the kinase domain of PINK1 in Pichia pastoris. Protein Expression and Purification, 2016, 128, 67-72.	1.3	5
79	Hypertonic Dextrose Stimulates Chondrogenic Cells to Deposit Collagen and Proliferate. Cartilage, 2021, , 194760352110145.	2.7	5
80	Overexpression of MEF2D contributes to oncogenic malignancy and chemotherapeutic resistance in ovarian carcinoma. American Journal of Cancer Research, 2019, 9, 887-905.	1.4	5
81	Crystal Structures of Ternary Complexes of MEF2 and NKX2–5 Bound to DNA Reveal a Disease Related Protein–Protein Interaction Interface. Journal of Molecular Biology, 2020, 432, 5499-5508.	4.2	3
82	Phenomena of weak electroluminescence of iron and other metal electrodes and their application potentiality in electrochemistry research. Electrochimica Acta, 1991, 36, 1591-1593.	5.2	2
83	Molecular Characterization, Spatial–Temporal Expression Profiles, and Injuryâ€responsive Regulation of Myocyteâ€specific Enhancer Factor 2 Gene Family in the Ricefield Eel, <i>Monopterus albus</i> . Journal of the World Aquaculture Society, 2018, 49, 396-411.	2.4	1
84	Novel Few-Shot Learning Neural Network for Predicting Carbohydrate-Active Enzyme Affinity Toward Fructo-Oligosaccharides. Journal of Computational Biology, 2021, 28, 1208-1218.	1.6	1
85	Structure-Based Approaches to Antigen-Specific Therapy of Myasthenia Gravis. , 2019, , .		0
86	NFAT and MEF2, Two Families of Calcium-dependent Transcription Regulators. , 2006, , 293-307.		0